

Differential Production Cross Section of Z Bosons as a Function of Transverse Momentum at $\sqrt{s} = 1.8$ TeV

B. Abbott,⁴⁵ M. Abolins,⁴² V. Abramov,¹⁸ B.S. Acharya,¹¹ I. Adam,⁴⁴ D.L. Adams,⁵⁴ M. Adams,²⁸ S. Ahn,²⁷ V. Akimov,¹⁶ G.A. Alves,² N. Amos,⁴¹ E.W. Anderson,³⁴ M.M. Baarmand,⁴⁷ V.V. Babintsev,¹⁸ L. Babukhadia,²⁰ A. Baden,³⁸ B. Baldin,²⁷ S. Banerjee,¹¹ J. Bantly,⁵¹ E. Barberis,²¹ P. Baringer,³⁵ J.F. Bartlett,²⁷ A. Belyaev,¹⁷ S.B. Beri,⁹ I. Bertram,¹⁹ V.A. Bezzubov,¹⁸ P.C. Bhat,²⁷ V. Bhatnagar,⁹ M. Bhattacharjee,⁴⁷ G. Blazey,²⁹ S. Blessing,²⁵ P. Bloom,²² A. Boehnlein,²⁷ N.I. Bojko,¹⁸ F. Borcharding,²⁷ C. Boswell,²⁴ A. Brandt,²⁷ R. Breedon,²² G. Briskin,⁵¹ R. Brock,⁴² A. Bross,²⁷ D. Buchholz,³⁰ V.S. Burtovoi,¹⁸ J.M. Butler,³⁹ W. Carvalho,³ D. Casey,⁴² Z. Casilum,⁴⁷ H. Castilla-Valdez,¹⁴ D. Chakraborty,⁴⁷ K.M. Chan,⁴⁶ S.V. Chekulaev,¹⁸ W. Chen,⁴⁷ D.K. Cho,⁴⁶ S. Choi,¹³ S. Chopra,²⁵ B.C. Choudhary,²⁴ J.H. Christenson,²⁷ M. Chung,²⁸ D. Claes,⁴³ A.R. Clark,²¹ W.G. Cobau,³⁸ J. Cochran,²⁴ L. Coney,³² W.E. Cooper,²⁷ D. Coppage,³⁵ C. Cretsinger,⁴⁶ D. Cullen-Vidal,⁵¹ M.A.C. Cummings,²⁹ D. Cutts,⁵¹ O.I. Dahl,²¹ K. Davis,²⁰ K. De,⁵² K. Del Signore,⁴¹ M. Demarteau,²⁷ D. Denisov,²⁷ S.P. Denisov,¹⁸ H.T. Diehl,²⁷ M. Diesburg,²⁷ G. Di Loreto,⁴² P. Draper,⁵² Y. Ducros,⁸ L.V. Dudko,¹⁷ S.R. Dugad,¹¹ A. Dyshkant,¹⁸ D. Edmunds,⁴² J. Ellison,²⁴ V.D. Elvira,⁴⁷ R. Engelmann,⁴⁷ S. Eno,³⁸ G. Eppley,⁵⁴ P. Ermolov,¹⁷ O.V. Eroshin,¹⁸ J. Estrada,⁴⁶ H. Evans,⁴⁴ V.N. Evdokimov,¹⁸ T. Fahland,²³ M.K. Fatyga,⁴⁶ S. Feher,²⁷ D. Fein,²⁰ T. Ferbel,⁴⁶ H.E. Fisk,²⁷ Y. Fisyrak,⁴⁸ E. Flattum,²⁷ G.E. Forden,²⁰ M. Fortner,²⁹ K.C. Frame,⁴² S. Fuess,²⁷ E. Gallas,²⁷ A.N. Galyaev,¹⁸ P. Gartung,²⁴ V. Gavrilov,¹⁶ T.L. Geld,⁴² R.J. Genik II,⁴² K. Genser,²⁷ C.E. Gerber,²⁷ Y. Gershtein,⁵¹ B. Gibbard,⁴⁸ G. Ginther,⁴⁶ B. Gobbi,³⁰ B. Gómez,⁵ G. Gómez,³⁸ P.I. Goncharov,¹⁸ J.L. González Solís,¹⁴ H. Gordon,⁴⁸ L.T. Goss,⁵³ K. Gounder,²⁴ A. Goussiou,⁴⁷ N. Graf,⁴⁸ P.D. Grannis,⁴⁷ D.R. Green,²⁷ J.A. Green,³⁴ H. Greenlee,²⁷ S. Grinstein,¹ P. Grudberg,²¹ S. Grünendahl,²⁷ G. Guglielmo,⁵⁰ J.A. Guida,²⁰ J.M. Guida,⁵¹ A. Gupta,¹¹ S.N. Gurzhiev,¹⁸ G. Gutierrez,²⁷ P. Gutierrez,⁵⁰ N.J. Hadley,³⁸ H. Haggerty,²⁷ S. Hagopian,²⁵ V. Hagopian,²⁵ K.S. Hahn,⁴⁶ R.E. Hall,²³ P. Hanlet,⁴⁰ S. Hansen,²⁷ J.M. Hauptman,³⁴ C. Hays,⁴⁴ C. Hebert,³⁵ D. Hedin,²⁹ A.P. Heinson,²⁴ U. Heintz,³⁹ R. Hernández-Montoya,¹⁴ T. Heuring,²⁵ R. Hirosky,²⁸ J.D. Hobbs,⁴⁷ B. Hoeneisen,⁶ J.S. Hoftun,⁵¹ F. Hsieh,⁴¹ Tong Hu,³¹ A.S. Ito,²⁷ S.A. Jerger,⁴² R. Jesik,³¹ T. Joffe-Minor,³⁰ K. Johns,²⁰ M. Johnson,²⁷ A. Jonckheere,²⁷ M. Jones,²⁶ H. Jöstlein,²⁷ S.Y. Jun,³⁰ S. Kahn,⁴⁸ D. Karmanov,¹⁷ D. Karmgard,²⁵ R. Kehoe,³² S.K. Kim,¹³ B. Klima,²⁷ C. Klopfenstein,²² B. Knuteson,²¹ W. Ko,²² J.M. Kohli,⁹ D. Koltick,³³ A.V. Kostritskiy,¹⁸ J. Kotcher,⁴⁸ A.V. Kotwal,⁴⁴ A.V. Kozelov,¹⁸ E.A. Kozlovsky,¹⁸ J. Krane,³⁴ M.R. Krishnaswamy,¹¹ S. Krzywdzinski,²⁷ M. Kubantsev,³⁶ S. Kuleshov,¹⁶ Y. Kulik,⁴⁷ S. Kunori,³⁸ F. Landry,⁴² G. Landsberg,⁵¹ A. Leflat,¹⁷ J. Li,⁵² Q.Z. Li,²⁷ J.G.R. Lima,³ D. Lincoln,²⁷ S.L. Linn,²⁵ J. Linnemann,⁴² R. Lipton,²⁷ J.G. Lu,⁴ A. Lucotte,⁴⁷ L. Lueking,²⁷ A.K.A. Maciel,²⁹ R.J. Madaras,²¹ R. Madden,²⁵ L. Magaña-Mendoza,¹⁴ V. Manankov,¹⁷ S. Mani,²² H.S. Mao,⁴ R. Markeloff,²⁹ T. Marshall,³¹ M.I. Martin,²⁷ R.D. Martin,²⁸ K.M. Mauritz,³⁴ B. May,³⁰ A.A. Mayorov,¹⁸ R. McCarthy,⁴⁷ J. McDonald,²⁵ T. McKibben,²⁸ J. McKinley,⁴² T. McMahon,⁴⁹ H.L. Melanson,²⁷ M. Merkin,¹⁷ K.W. Merritt,²⁷ C. Miao,⁵¹ H. Miettinen,⁵⁴ A. Mincer,⁴⁵ C.S. Mishra,²⁷ N. Mokhov,²⁷ N.K. Mondal,¹¹ H.E. Montgomery,²⁷ M. Mostafa,¹ H. da Motta,² F. Nang,²⁰ M. Narain,³⁹ V.S. Narasimham,¹¹ A. Narayanan,²⁰ H.A. Neal,⁴¹ J.P. Negret,⁵ P. Nemethy,⁴⁵ D. Norman,⁵³ L. Oesch,⁴¹ V. Oguri,³ N. Oshima,²⁷ D. Owen,⁴² P. Padley,⁵⁴ A. Para,²⁷ N. Parashar,⁴⁰ Y.M. Park,¹² R. Partridge,⁵¹ N. Parua,⁷ M. Paterno,⁴⁶ B. Pawlik,¹⁵ J. Perkins,⁵² M. Peters,²⁶ R. Piegaia,¹ H. Piekarczyk,²⁵ Y. Pischalnikov,³³ B.G. Pope,⁴² H.B. Prosper,²⁵ S. Protopopescu,⁴⁸ J. Qian,⁴¹ P.Z. Quintas,²⁷ R. Raja,²⁷ S. Rajagopalan,⁴⁸ O. Ramirez,²⁸ N.W. Reay,³⁶ S. Reucroft,⁴⁰ M. Rijssenbeek,⁴⁷ T. Rockwell,⁴² M. Roco,²⁷ P. Rubinov,³⁰ R. Ruchti,³² J. Rutherford,²⁰ A. Sánchez-Hernández,¹⁴ A. Santoro,² L. Sawyer,³⁷ R.D. Schamberger,⁴⁷ H. Schellman,³⁰ J. Sculli,⁴⁵ E. Shabalina,¹⁷ C. Shaffer,²⁵ H.C. Shankar,¹¹ R.K. Shivpuri,¹⁰ D. Shpakov,⁴⁷ M. Shupe,²⁰ R.A. Sidwell,³⁶ H. Singh,²⁴ J.B. Singh,⁹ V. Sirotenko,²⁹ P. Slattey,⁴⁶ E. Smith,⁵⁰ R.P. Smith,²⁷ R. Snihur,³⁰ G.R. Snow,⁴³ J. Snow,⁴⁹ S. Snyder,⁴⁸ J. Solomon,²⁸ X.F. Song,⁴ M. Sosebee,⁵² N. Sotnikova,¹⁷ M. Souza,² N.R. Stanton,³⁶ G. Steinbrück,⁵⁰ R.W. Stephens,⁵² M.L. Stevenson,²¹ F. Stichelbaut,⁴⁸ D. Stoker,²³ V. Stolin,¹⁶ D.A. Stoyanova,¹⁸ M. Strauss,⁵⁰ K. Streets,⁴⁵ M. Strovink,²¹ A. Sznajder,³ P. Tamburello,³⁸ J. Tarazi,²³ M. Tartaglia,²⁷ T.L.T. Thomas,³⁰ J. Thompson,³⁸ D. Toback,³⁸ T.G. Trippe,²¹ P.M. Tuts,⁴⁴ V. Vaniev,¹⁸ N. Varelas,²⁸ E.W. Varnes,²¹ A.A. Volkov,¹⁸ A.P. Vorobiev,¹⁸ H.D. Wahl,²⁵ J. Warchol,³² G. Watts,⁵¹ M. Wayne,³² H. Weerts,⁴² A. White,⁵² J.T. White,⁵³ J.A. Wightman,³⁴ S. Willis,²⁹ S.J. Wimpenny,²⁴ J.V.D. Wirjawan,⁵³ J. Womersley,²⁷ D.R. Wood,⁴⁰ R. Yamada,²⁷ P. Yamin,⁴⁸ T. Yasuda,²⁷ P. Yepes,⁵⁴ K. Yip,²⁷ C. Yoshikawa,²⁶ S. Youssef,²⁵ J. Yu,²⁷ Y. Yu,¹³ M. Zanabria,⁵ Z. Zhou,³⁴ Z.H. Zhu,⁴⁶ M. Zielinski,⁴⁶ D. Zieminska,³¹ A. Zieminski,³¹ V. Zutshi,⁴⁶ E.G. Zverev,¹⁷ and A. Zylberstejn⁸

(DØ Collaboration)

- ¹ *Universidad de Buenos Aires, Buenos Aires, Argentina*
² *LAFEX, Centro Brasileiro de Pesquisas Físicas, Rio de Janeiro, Brazil*
³ *Universidade do Estado do Rio de Janeiro, Rio de Janeiro, Brazil*
⁴ *Institute of High Energy Physics, Beijing, People's Republic of China*
⁵ *Universidad de los Andes, Bogotá, Colombia*
⁶ *Universidad San Francisco de Quito, Quito, Ecuador*
⁷ *Institut des Sciences Nucléaires, IN2P3-CNRS, Université de Grenoble 1, Grenoble, France*
⁸ *DAPNIA/Service de Physique des Particules, CEA, Saclay, France*
⁹ *Panjab University, Chandigarh, India*
¹⁰ *Delhi University, Delhi, India*
¹¹ *Tata Institute of Fundamental Research, Mumbai, India*
¹² *Kyungshung University, Pusan, Korea*
¹³ *Seoul National University, Seoul, Korea*
¹⁴ *CINVESTAV, Mexico City, Mexico*
¹⁵ *Institute of Nuclear Physics, Kraków, Poland*
¹⁶ *Institute for Theoretical and Experimental Physics, Moscow, Russia*
¹⁷ *Moscow State University, Moscow, Russia*
¹⁸ *Institute for High Energy Physics, Protvino, Russia*
¹⁹ *Lancaster University, Lancaster, United Kingdom*
²⁰ *University of Arizona, Tucson, Arizona 85721*
²¹ *Lawrence Berkeley National Laboratory and University of California, Berkeley, California 94720*
²² *University of California, Davis, California 95616*
²³ *University of California, Irvine, California 92697*
²⁴ *University of California, Riverside, California 92521*
²⁵ *Florida State University, Tallahassee, Florida 32306*
²⁶ *University of Hawaii, Honolulu, Hawaii 96822*
²⁷ *Fermi National Accelerator Laboratory, Batavia, Illinois 60510*
²⁸ *University of Illinois at Chicago, Chicago, Illinois 60607*
²⁹ *Northern Illinois University, DeKalb, Illinois 60115*
³⁰ *Northwestern University, Evanston, Illinois 60208*
³¹ *Indiana University, Bloomington, Indiana 47405*
³² *University of Notre Dame, Notre Dame, Indiana 46556*
³³ *Purdue University, West Lafayette, Indiana 47907*
³⁴ *Iowa State University, Ames, Iowa 50011*
³⁵ *University of Kansas, Lawrence, Kansas 66045*
³⁶ *Kansas State University, Manhattan, Kansas 66506*
³⁷ *Louisiana Tech University, Ruston, Louisiana 71272*
³⁸ *University of Maryland, College Park, Maryland 20742*
³⁹ *Boston University, Boston, Massachusetts 02215*
⁴⁰ *Northeastern University, Boston, Massachusetts 02115*
⁴¹ *University of Michigan, Ann Arbor, Michigan 48109*
⁴² *Michigan State University, East Lansing, Michigan 48824*
⁴³ *University of Nebraska, Lincoln, Nebraska 68588*
⁴⁴ *Columbia University, New York, New York 10027*
⁴⁵ *New York University, New York, New York 10003*
⁴⁶ *University of Rochester, Rochester, New York 14627*
⁴⁷ *State University of New York, Stony Brook, New York 11794*
⁴⁸ *Brookhaven National Laboratory, Upton, New York 11973*
⁴⁹ *Langston University, Langston, Oklahoma 73050*
⁵⁰ *University of Oklahoma, Norman, Oklahoma 73019*
⁵¹ *Brown University, Providence, Rhode Island 02912*
⁵² *University of Texas, Arlington, Texas 76019*
⁵³ *Texas A&M University, College Station, Texas 77843*
⁵⁴ *Rice University, Houston, Texas 77005*

We present a measurement of the transverse momentum distribution of Z bosons produced in $p\bar{p}$ collisions at $\sqrt{s} = 1.8$ TeV using data collected by the DØ experiment at the Fermilab Tevatron Collider during 1994–1996. We find good agreement between our data and a current resummation calculation. We also use our data to extract values of the non-perturbative parameters for a particular version of the resummation formalism, obtaining significantly more precise values than previous determinations.

We report a new measurement [1,2] of the differential cross section with respect to transverse momentum ($d\sigma/dp_T$) of the Z boson in the dielectron channel with statistics and precision greatly improved beyond previous measurements [3,4]. The measurement of $d\sigma/dp_T$ of the Z boson provides a sensitive test of QCD at high- Q^2 . At small transverse momentum (p_T), where the cross section is highest, uncertainties in the phenomenology of vector boson production have contributed significantly to the uncertainty in the mass of the W boson. Due to its similar production characteristics and the fact that the decay electrons can be very well-measured, the Z provides a good laboratory for evaluating the phenomenology of vector boson production.

In the parton model, Z bosons are produced in collisions of $q\bar{q}$ constituents of the proton and antiproton. The fact that observed Z bosons have finite p_T can be attributed to gluon radiation from the colliding partons prior to their annihilation. In standard perturbative QCD (pQCD), the cross section for Z boson production is calculated by expanding in powers of the strong coupling constant, α_s . This procedure works well when $p_T^2 \sim Q^2$ with $Q = M_Z$. However, when $p_T \ll Q$, correction terms that are proportional to $\alpha_s \ln(Q^2/p_T^2)$ become significant, and the cross section diverges at small p_T . This difficulty is surmounted by reordering the perturbative series through a technique called *resummation* [5–13]. Although this technique extends the applicability of pQCD to lower values of p_T , a more fundamental barrier is encountered when p_T approaches Λ_{QCD} . In this region, α_s becomes large and the perturbative calculation is no longer valid. In order to account for the non-perturbative contribution, a phenomenological form factor must be invoked, which contains several parameters that must be tuned to data [8,10,11].

The resummation may be carried out in impact-parameter (b) space via a Fourier transform, or in transverse momentum space. Both formalisms require a non-perturbative function to describe the low- p_T region beyond some cut-off value b_{max} or p_{Tlim} and they merge to the fixed-order perturbation theory at $p_T \sim Q$. The current state-of-the-art for the b -space formalism resums terms to next-to-next-to-next-to-leading-log and includes fixed-order terms to $\mathcal{O}(\alpha_s^2)$ [11]. Similarly, the p_T -space formalism resums terms to next-to-next-to-leading-log and includes fixed-order terms to $\mathcal{O}(\alpha_s)$ [13].

In the b -space formalism, the resummed cross section is modified at large b (above b_{max}) by $\exp(-S_{\text{NP}}(b, Q^2))$. The form factor $S_{\text{NP}}(b, Q^2)$ has a general renormalization group invariant form, but requires a specific choice of parameterization when making predictions. A possible choice, suggested by Ladinsky and Yuan [11], is

$$S_{\text{NP}}(b, Q^2) = g_1 b^2 + g_2 b^2 \ln\left(\frac{Q^2}{Q_0^2}\right) + g_1 g_3 b \ln(100 x_i x_j), \quad (1)$$

where x_i and x_j are the fractions of incident hadron momenta carried by the colliding partons and g_i are the non-perturbative parameters. An earlier parameterization by Davies, Webber, and Stirling [8] corresponds to the above with $g_3 \equiv 0$. For measurements at the Fermilab Tevatron at $Q^2 = M_Z^2$, the calculation is most sensitive to the value of g_2 and quite insensitive to the value of g_3 .

In the p_T -space formalism, the resummed cross section is modified at low- p_T (below p_{Tlim}) by multiplying the cross section by $F_{\text{NP}}(p_T)$. In this case, the form of the non-perturbative function is not constrained by renormalization group invariance. The choice suggested by Ellis and Veseli [13], is

$$\tilde{F}_{\text{NP}}(p_T) = 1 - e^{-\tilde{a} p_T^2} \quad (2)$$

where \tilde{a} is a non-perturbative parameter.

Previously published measurements of the differential cross section for Z boson production have been limited primarily by statistics (candidate samples of a few hundred events). This measurement is based on a sample of 6407 $Z \rightarrow e^+e^-$ events, corresponding to an integrated luminosity of $\approx 111 \text{ pb}^{-1}$, collected with the DØ detector [14] in 1994-1996. A recent measurement by the CDF Collaboration has a similar number of events [15].

Electrons are detected in the uranium/liquid-argon calorimeter with a fractional energy resolution of $\approx 15\%/\sqrt{E(\text{GeV})}$. The calorimeter has a transverse granularity at the electron shower maximum of $\Delta\eta \times \Delta\phi = 0.05 \times 0.05$, where η is the pseudorapidity and ϕ is the azimuthal angle. The two electron candidates in the event with the highest transverse energy (E_T), both having $E_T > 25 \text{ GeV}$, are used to reconstruct the Z boson candidate. One electron is required to be in the central region, $|\eta_{\text{det}}| < 1.1$, and the second electron may be either in the central or in the forward region, $1.5 < |\eta_{\text{det}}| < 2.5$, where η_{det} refers to the value of η obtained by assuming that the shower originates from the center of the detector. Offline, both electrons are required to be isolated and to satisfy cluster-shape requirements. Additionally, at least one of the electrons is required to have a matching track in the drift chamber system that points to the reconstructed calorimeter cluster.

Both the acceptance and the theory predictions modified by the DØ detector resolution are calculated using a simulation technique originally developed for measuring the mass of the W boson [16], with minor modifications required by changes in selection criteria. The four-momentum of the Z boson is obtained by generating the mass of the Z according to an energy-dependent Breit-Wigner lineshape.

The p_T and rapidity of the Z boson are chosen randomly from two-dimensional grids created using the computer program LEGACY [12], which calculates the Z boson cross section for a given p_T , rapidity, and mass of the Z boson. The positions and energies of the electrons are smeared according to the measured resolutions, and corrected for offsets in energy scale caused by the underlying event and recoil particles that overlap the calorimeter towers. Underlying events are modeled using data from random inelastic $p\bar{p}$ collisions of the same luminosity profile as the Z boson sample. The electron energy and angular resolutions are tuned to reproduce the observed width of the mass distribution at the Z -boson resonance and the difference between the reconstructed vertex positions of the electrons.

We determine the shape of the efficiency of the event selection criteria as a function of p_T using $Z \rightarrow e^+e^-$ events generated with HERWIG [17], smeared with the $D\emptyset$ detector resolutions, and overlaid on randomly selected zero bias $p\bar{p}$ collisions. This simulation models the effects of the underlying event and jet activity on the selection of the electrons. The absolute efficiency is obtained from $Z \rightarrow e^+e^-$ data [18]. The values of the efficiency times acceptance range from 26-37% for p_T below 200 GeV and is 53% for p_T above 200 GeV.

The primary background arises from multiple-jet production from QCD processes in which two jets pass the electron selection criteria. We use several $D\emptyset$ data sets for estimating this background—direct- γ events, dijet events, and dielectron events in which both electrons fail quality criteria—all of which have very similar kinematic characteristics [1]. The level of the multijet background is determined by fitting the ee invariant mass in the range $60 < M_{ee} < 120$ GeV to a linear combination of Monte Carlo $Z \rightarrow e^+e^-$ signal events (using PYTHIA [19]) and background (from direct- γ events). We assign a systematic uncertainty to this measurement by varying the choice of mass window used in the fit, and by changing the background sample among those mentioned above. We estimate the total multijet background level to be $(4.4 \pm 0.9)\%$. The direct- γ sample is used to parameterize the shape of the background distribution as a function of p_T . Backgrounds from other sources, such as $Z \rightarrow \tau^+\tau^-$, $t\bar{t}$, and diboson production, are negligible.

We use the data corrected for background, acceptance, and efficiency, to determine the best value of the non-perturbative parameter, g_2 , given our data. In the fit, we fix g_1 and g_3 to the values obtained in [11] and vary the value of g_2 . We use the CTEQ4M pdf. The prediction is smeared with the known detector resolutions, and the result fitted to our data. The resulting χ^2 distribution as a function of g_2 is well-behaved and parabolic, yielding a value

of $g_2 = 0.59 \pm 0.06$ GeV², considerably more precise than previous determinations. For completeness, we also fit the individual values of g_1 and g_3 , with the other two parameters fixed to their published values [11]. We obtain $g_1 = 0.09 \pm 0.03$ GeV² and $g_3 = -1.1 \pm 0.6$ GeV⁻¹. Both results are consistent with the values of Ref. [11].

To determine the true $d\sigma/dp_T$, we correct the measured cross section for effects of detector smearing, using the ratio of generated to resolution-smeared ansatz p_T distributions. We use the calculation from LEGACY as our ansatz function, with the g_2 determined from our fit. The largest smearing correction occurs at low- p_T , where smearing causes the largest fractional change in p_T and where the kinematic boundary at $p_T = 0$ produces non-Gaussian smearing. The correction is 18.5% in the first bin, decreasing to about 2% at 5 GeV. For all p_T values above 5 GeV, the correction is $\lesssim 5\%$. Systematic uncertainties arising from the choice of ansatz function are evaluated by varying g_2 within ± 1 standard deviation of the best-fit values. Additional uncertainties are evaluated by varying the detector resolutions by ± 1 standard deviation from the nominal values. The effect of these variations is negligible relative to the other uncertainties in the measurement.

Table I shows the values of $d\sigma(Z \rightarrow e^+e^-)/dp_T$. The uncertainties on the data points include statistical and systematic contributions. An additional normalization uncertainty of $\pm 4.4\%$ arises from the uncertainty on the integrated luminosity [18] that is not included in any of the plots nor in the table, but must be taken into account in any fits involving an absolute normalization.

Figure 1 shows the final differential cross section, corrected for the $D\emptyset$ detector resolutions, compared to the fixed-order calculation and the resummation calculation with three different parameterizations of the non-perturbative region using published values of the non-perturbative parameters. Also shown are the fractional differences of the data from the considered resummation predictions. The data are normalized to the measured $Z \rightarrow e^+e^-$ cross section (221 pb [18]) and the predictions are absolutely normalized. We observe the best agreement with the Ladinsky-Yuan parameters for the b -space formalism; however, we expect that fits to the data using the Davies-Weber-Stirling (b -space) or Ellis-Veseli (p_T -space) parameterizations of the non-perturbative functions could describe the data similarly well.

Figure 2 shows the measured differential cross section compared to the fixed-order calculation and the resummation calculation using the Ladinsky-Yuan parameterization. We observe strong disagreement between the data and the fixed-order prediction in the shape for all but the highest values of p_T . We at-

p_T range (GeV)	nominal p_T value (GeV)	number of events	$d\sigma(Z \rightarrow e^+e^-)/dp_T$ (pb/GeV)
0-1	0.6	156	6.04±0.53
1-2	1.5	424	16.2±0.96
2-3	2.5	559	20.4±1.1
3-4	3.5	572	19.7±1.1
4-5	4.5	501	16.2±0.92
5-6	5.5	473	15.0±0.87
6-7	6.5	440	14.1±0.84
7-8	7.5	346	11.1±0.73
8-9	8.5	312	10.0±0.69
9-10	9.5	285	9.29±0.67
10-12	11.0	439	7.25±0.54
12-14	13.0	326	5.45±0.44
14-16	15.0	258	4.45±0.39
16-18	17.0	203	3.54±0.33
18-20	19.0	181	3.21±0.31
20-25	22.3	287	2.06±0.18
25-30	27.3	174	1.29±0.13
30-35	32.3	124	0.962±0.11
35-40	37.4	104	0.840±0.10
40-50	44.5	92	0.373±0.045
50-60	54.5	61	0.251±0.036
60-70	64.5	40	0.163±0.027
70-85	76.6	20	0.053±0.012
85-100	91.7	13	0.034±0.009
100-200	135	15	0.0050±0.0013
200-300	228	2	0.0004 ^{+0.0004} _{-0.0003}

TABLE I. Summary of the results of the measurement of the p_T distribution of the Z boson. The range of p_T corresponds to the intervals used for binning the data. The nominal p_T corresponds to the value of p_T used to plot the data and was obtained from theory. The quantity $d\sigma(Z \rightarrow e^+e^-)/dp_T$ corresponds to the differential cross section in each bin of p_T for $Z \rightarrow e^+e^-$ production. The uncertainty on the differential cross section includes both systematic and statistical uncertainties, but does not include overall normalization uncertainty due to the luminosity of $\pm 4.4\%$.

tribute this to the divergence of the next-to-leading-order calculation at $p_T=0$, and a significant enhancement of the cross section relative to the prediction at moderate values of p_T . This disagreement confirms the presence of contributions from soft gluon emission, which are accounted for in the resummation formalisms.

In summary, we have measured the inclusive differential cross section of the Z boson as a function of its transverse momentum. With the enhanced precision of this measurement over those previous, we can probe non-perturbative, resummation, and fixed-order QCD effects. We observe good agreement between the b -space resummation calculation using the published values of the non-perturbative parameters from Ladinsky-Yuan and the measure-

ment for all values of p_T . Using their parameterization for the non-perturbative region, we obtain $g_2 = 0.59 \pm 0.06 \text{ GeV}^2$.

We thank the Fermilab and collaborating institution staffs for contributions to this work and acknowledge support from the Department of Energy and National Science Foundation (USA), Commissariat à l'Énergie Atomique (France), Ministry for Science and Technology and Ministry for Atomic Energy (Russia), CAPES and CNPq (Brazil), Departments of Atomic Energy and Science and Education (India), Colciencias (Colombia), CONACyT (Mexico), Ministry of Education and KOSEF (Korea), and CONICET and UBACyT (Argentina).

-
- [1] DØ Collaboration, B. Abbott *et al.*, submitted to Phys. Rev. D., FERMILAB PUB-99/197-E, hep-ex/9907009.
 - [2] D. Casey, Ph.D. thesis, University of Rochester, 1997 (unpublished), http://www-d0.fnal.gov/publications_talks/thesis/casey/thesis.ps.
 - [3] UA2 Collaboration, P. Bagnaia *et al.*, Z. Phys. C **47**, 523 (1990).
 - [4] CDF Collaboration, F. Abe *et al.*, Phys. Rev. Lett. **67**, 2937 (1991).
 - [5] J.C. Collins, D.E. Soper, Nucl. Phys. **B193**, 381 (1981); **B213**, 545E (1983); J.C. Collins, D.E. Soper, G. Sterman, *ibid.* **B250**, 199 (1985).
 - [6] C.T.H. Davies and W.J. Stirling, Nucl. Phys. **B244**, 337 (1984).
 - [7] G. Altarelli, R.K. Ellis, M. Greco, and G. Martinelli, Nucl. Phys. **B246**, 12 (1984).
 - [8] C.T.H. Davies, B.R. Weber, W.J. Stirling, Nucl. Phys. **B256**, 413 (1985).
 - [9] P.B. Arnold and M.H. Reno, Nucl. Phys. **B319**, 37 (1989); **B330**, 284E (1990).
 - [10] P.B. Arnold and R.P. Kaufman, Nucl. Phys. **B349**, 381 (1991).
 - [11] G.A. Ladinsky and C.-P. Yuan, Phys. Rev. D **50**, 4239 (1994).
 - [12] C. Balazs and C.-P. Yuan, Phys. Rev. D **56**, 5558 (1997).
 - [13] R.K. Ellis, S. Veseli, Nucl. Phys. **B511**, 649 (1998).
 - [14] DØ Collaboration, S. Abachi *et al.*, Nucl. Instr. and Methods in Phys. Res. A **338**, 185 (1994).
 - [15] CDF Collaboration, T. Affolder *et al.*, submitted to Phys. Rev. Lett., FERMILAB PUB-99/220-E.
 - [16] DØ Collaboration, B. Abbott *et al.*, Phys. Rev. D **58**, 092003 (1998).
 - [17] G. Marchesini *et al.*, Comput. Phys. Commun. **67**, 465 (1992).
 - [18] DØ Collaboration, B. Abbott *et al.*, submitted to Phys. Rev. D., FERMILAB PUB-99/171-E, hep-ex/9906025.
 - [19] H.U. Bengtsson and T. Sjostrand, Comput. Phys. Commun. **46**, 43 (1987).

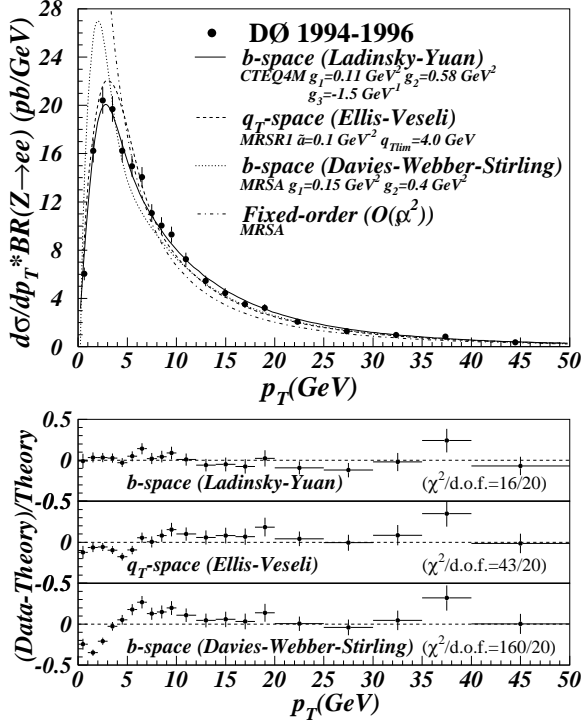


FIG. 1. The differential cross section as a function of p_T compared to the resummation calculation with three different published parameterizations of the non-perturbative region and to the fixed-order calculation. Also shown are the fractional differences between the data and each of the resummation predictions.

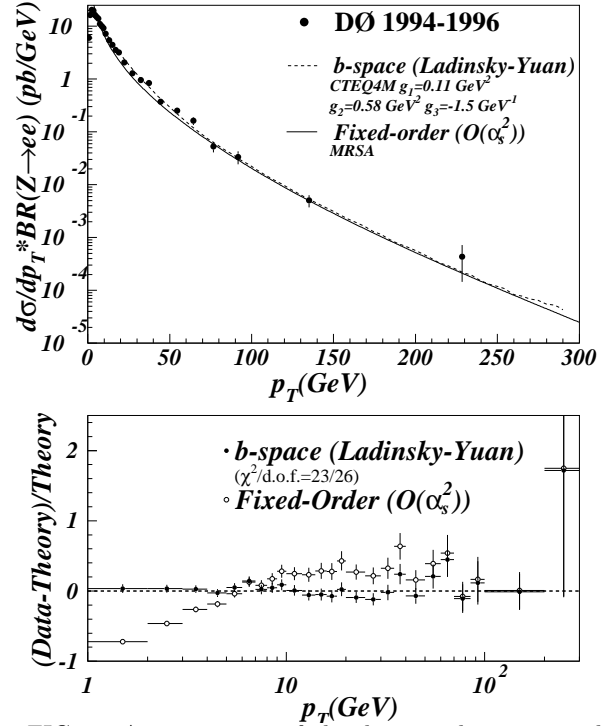


FIG. 2. A comparison of the data to the resummed and fixed-order ($\mathcal{O}(\alpha_s^2)$) calculations. Also shown are the fractional differences between the data and the resummed and fixed-order calculations. The uncertainties shown include both statistical and systematic uncertainties (other than an overall normalization uncertainty due to the luminosity uncertainty).